PGE_2 Activation of Apical Membrane Cl^- Channels in A6 Epithelia: Impedance Analysis

Teodor G. Păunescu and Sandy I. Helman
Department of Molecular and Integrative Physiology, University of Illinois at Urbana-Champaign, Urbana, Illinois 61801 USA

ABSTRACT Measurements of transepithelial electrical impedance of continuously short-circuited A6 epithelia were made at audio frequencies (0.244 Hz to 10.45 kHz) to investigate the time course and extent to which prostaglandin E_2 (PGE_2) modulates Cl^- transport and apical membrane capacitance in this cell-cultured model epithelium. Apical and basolateral membrane resistances were determined by nonlinear curve-fitting of the impedance vectors at relatively low frequencies (<50 Hz) to equations (Păunescu, T. G., and S. I. Helman. 2001. *Biophys. J.* 81:838–851) where depressed Nyquist impedance semicircles were characteristic of the membrane impedances under control Na^+-transporting and amiloride-inhibited conditions. In all tissues (control, amiloride-blocked, and amiloride-blocked and furosemide-pretreated), PGE_2 caused relatively small (<~3 $\mu A/cm^2$) and rapid (<60 s) maximal increase of chloride current due to activation of a rather large increase of apical membrane conductance that preceded significant activation of Na^+ transport through amiloride-sensitive epithelial Na^+ channels (ENaCs). Apical membrane capacitance was frequency-dependent with a Cole-Cole dielectric dispersion whose relaxation frequency was near 150 Hz. Analysis of the time-dependent changes of the complex frequency-dependent equivalent capacitance of the cells at frequencies >1.5 kHz revealed that the mean 9.8% increase of capacitance caused by PGE_2 was not correlated in time with activation of chloride conductance, but rather correlated with activation of apical membrane Na^+ transport.

INTRODUCTION

In experiments designed to study hormonal regulation of Na^+ transport in epithelial tissues, the activation of chloride transport in addition to sodium transport imposes complexities in the design of experiments and interpretation of data unlike those encountered in studies of frog skin and toad urinary bladder where adenosine 3′,5′-cyclic monophosphate (cAMP) selectively activates apical membrane amiloride-sensitive epithelial Na^+ channels (ENaCs) (Els and Helman, 1981, 1997; Schlondorff and Satriano, 1985). To understand the complexities to be encountered in studies of cell-cultured A6 epithelia where cAMP activates both Na^+ and Cl^- channels, we turned to noninvasive methods of impedance analysis to determine the time course and magnitude of change of apical membrane conductance to chloride and apical membrane capacitance in response to elevation of intracellular cAMP by forskolin and prostaglandin E_2 (PGE_2) that are known to elevate cAMP in target tissues (Chalfant et al., 1993; Hall et al., 1976; Sonnenburg and Smith, 1988; Yanase and Handler, 1986; Noland et al., 1992).

Although the measurement of transepithelial impedance is in principle straightforward, previous studies from our laboratory had indicated that the dielectric properties of epithelial plasma membranes may exhibit α-dielectric dispersions at audio frequencies (Awayda et al., 1999; Liu and Helman, 1998; Păunescu and Helman, 2000) that complicate measurement of plasma membrane capacitance. The theoretical principles and considerations relevant to the present studies have been discussed elsewhere (Păunescu and Helman, 2001) where we examined the contributions of Maxwell-Wagner-like and Cole-Cole dielectric dispersions to the transepithelial impedance locus of the series arrangement of apical and basolateral membrane impedances that are paralleled electrically by paracellular shunt resistances.

Evaluation of the time-dependent changes of short-circuit current and transepithelial impedance has led us to conclude that PGE_2 maximally activates a rather large apical membrane chloride conductance in <1 min. Activation of chloride channels preceded activation of the apical membrane sodium conductance from basal states where chloride conductance was immeasurably small or absent in A6 epithelia grown on Transwell-clear inserts. Because the time-dependent increases of apical membrane capacitance paralleled the increases of sodium transport and were completely dissociated from those of activation of chloride conductance, we concluded that the slightly delayed and relatively slow increases of capacitance were associated with activation of apical membrane sodium conductance.

Received for publication 19 September 2000 and in final form 26 April 2001.

Address reprint requests to Dr. Sandy I. Helman, Dept. of Molecular and Integrative Physiology, University of Illinois at Urbana-Champaign, 524 Burill Hall, 407 S. Goodwin Ave., Urbana, IL 61801-3796. Tel.: 217-333-7913; Fax: 217-333-1133; E-mail: s-helman@uiuc.edu.

0006-3495/01/08/852/15 $2.00

MATERIALS AND METHODS

Tissues, solutions, and drugs

A6 cells at passages 109 to 114 were used in the present studies. After growth on 75 cm^2 plastic culture flasks at 28°C in a humidified incubator containing 1% CO_2, the cells were subcultured on Transwell-clear cluster inserts (Costar, Cambridge, MA) for at least 14 days to achieve confluence and development of their transepithelial transport characteristics (Helman

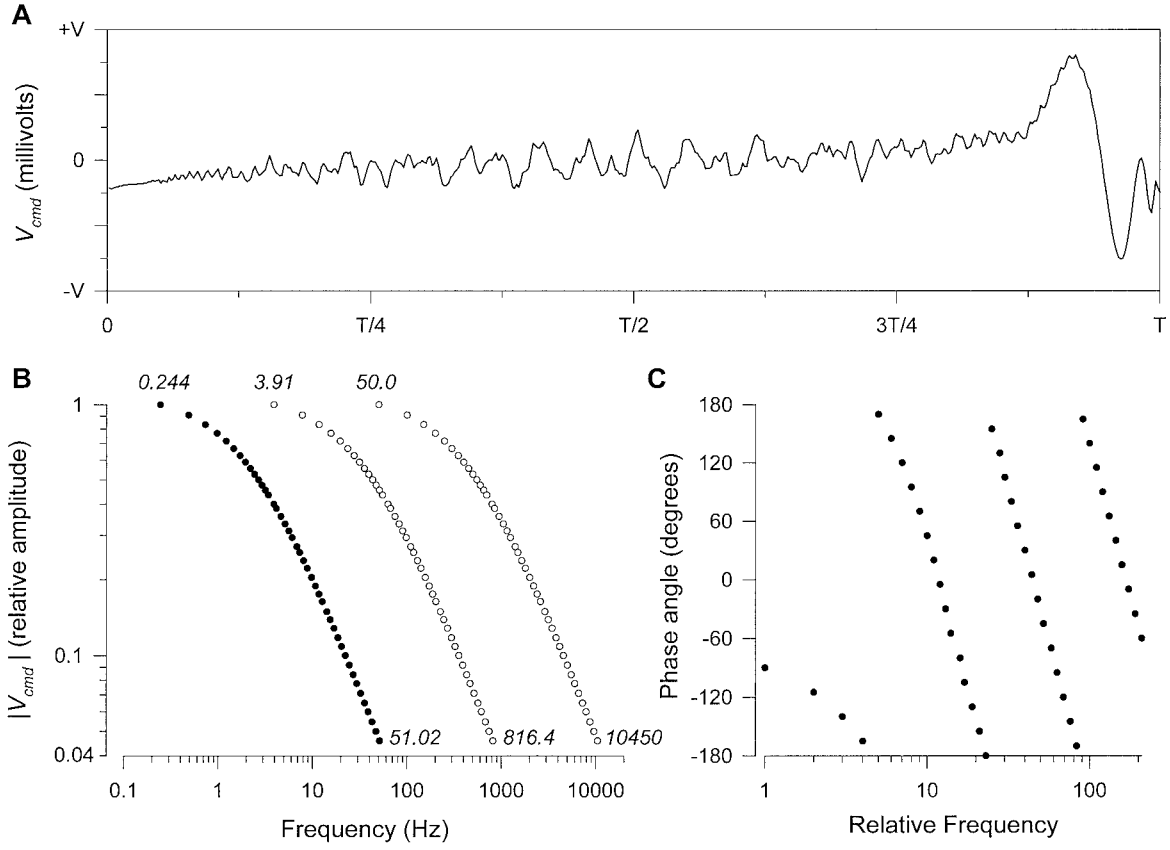

FIGURE 1 (*A*) Composite voltage command signal, V_{cmd}, consisted of the vectorial sum of 43 sinusoids with relative amplitudes (*B*) and phase angles (*C*) and with time periods, *T*, determined by their fundamental frequencies (0.244, 3.91, and 50.0 Hz).

and Liu, 1997). The tissues were fed twice weekly with a Cl^--rich growth medium that was based on a mixture of equal parts of Ham's nutrient mixture F-12 with L-glutamine and without sodium bicarbonate (N-6760, Sigma Chemical Co., St. Louis, MO) and L-15 Leibovitz medium (L-4386, Sigma Chemical Co.). This mixture was supplemented with 10% fetal bovine serum (FBS) (SH0070, HyClone, Logan, UT), 2.57 mM sodium bicarbonate, 3.84 mM L-glutamine (Sigma Chemical Co.), 96 U/ml penicillin, and 96 μg/ml streptomycin (BioWhittaker, Walkersville, MD).

The tissues were transferred to edge damage-free chambers (Abramcheck et al., 1985; Awayda et al., 1999) and short-circuited for the duration of the experiments using a very low-noise, four-electrode (Ag/AgCl, 4.5 M NaCl, 3% agar) voltage clamp while being perfused continuously at flow rates of ~7 ml/min through chamber volumes of ~0.5 ml with the growth medium without FBS and glutamine. Na^+, K^+, Cl^-, Ca^{2+}, and Mg^{2+} concentrations were 103.0, 3.34, 106.8, 0.59, and 0.91 mM, respectively. Short-circuit currents (I_{sc}) were allowed to stabilize for at least 2 h before onset of experimental periods. Characteristically, the I_{sc} increased transiently when tissues were initially short-circuited, returning to near steady-state values within 1 to 2 h (Păunescu et al., 1997); 100 μM amiloride added to the apical perfusion solution was used to inhibit blocker-sensitive Na^+ currents (I_{Na}^{bs}).

To elevate intracellular cAMP, forskolin (Sigma Chemical Co.) or prostaglandin E_2 (PGE_2) (Sigma Chemical Co.) was added to the basolateral perfusion solution at final concentrations of 25 μM or 1 μM, respectively. Stock solutions of forskolin and PGE_2 were dissolved in ethanol at 10^{-2} M and stored at -20°C. Furosemide (Sigma Chemical Co.) was added directly to the basolateral solution at 1 mM to inhibit electroneutral chloride transport at the basolateral membranes of the cells (Brazy and Gunn, 1976; Lambert and Lowe, 1980; Stoddard et al., 1985). A chloride-free, gluconate Ringer's solution containing 100 mM sodium gluconate, 2.4 mM $KHCO_3$, and 2.0 mM $CaSO_4$ was perfused through apical and basolateral chambers in those experiments where tissues were exposed for 1 h during control periods and chronically thereafter to chloride-free solution.

Impedance analysis

Transepithelial impedance was measured under voltage clamp conditions using three overlapping bands of frequencies (low, medium, and high) between 0.244 Hz and 10.45 kHz (Fig. 1) and using essentially the same approach described previously (Awayda et al., 1999), but with several modifications. The voltage command signals (V_{cmd}) consisted of the vectorial sum of 43 frequencies where the absolute amplitude of each sinusoid decreased with increasing frequency (Fig. 1 *B*) and with the phase angle indicated in Fig. 1 *C*. This design of the composite voltage command signal served to assure that the capacitive currents at each frequency would be closer in magnitude than would occur if the amplitudes of the voltage command sinusoids were of equal amplitude at all frequencies. With fundamental periods (*T*) of 4.098 s (low frequencies), 255.7 ms (medium frequencies), and 20 ms (high frequencies), corresponding to fundamental frequencies of 0.244, 3.91, and 50.0 Hz, the relative amplitudes of the voltage command sinusoids in all three frequency bands can be compared (Fig. 1 *B*), especially in the overlapping ranges of frequency between bands (3.91 to 51.02 Hz and 50.0 to 816.4 Hz). Consequently, impedance in the overlapping bands of frequency was measured with sinusoids of markedly differing voltage and current amplitudes at each time point of measurement, thereby providing a built-in check for testing and assuring that

impedance was independent of the magnitude of V_{cmd}. The magnitudes of V_{cmd} (Fig. 1 *A*) were adjusted so that the peak-to-peak changes of transepithelial voltage were near 2 mV. Consequently, it could be assumed that impedance was measured for all practical purposes in linear ranges of the current-voltage relationships of the channels.

An IBM-compatible computer containing a DSP2200 board (16 bit ADCs, 16 bit DACs, National Instruments, Austin, TX) was programmed using LabWindows for DOS to output the analog V_{cmd} signals and to simultaneously digitize the measured transepithelial voltage and current signals after amplification and filtration at the Nyquist frequencies. Low, medium, and high frequency bands were each output in sequence over four time periods and data collection for analysis was retained for only the last period of each band. Accordingly, the total time for data acquisition was near 5.2 s [4.098 + (4 × 0.2557) + (4 × 0.020)]. These signals were Fourier-transformed to yield the voltage and current vectors. Z_{meas} was calculated as the quotient of voltage and current vectors at the respective frequencies. Where appropriate, data were normalized to planar surface area and plotted as Nyquist (ReZ_{meas} vs. ImZ_{meas}) or Bode plots ($|Z_{meas}|$ and phase angle versus frequency). See Results for calculations of apical and basolateral membrane resistances and capacitances.

Data are summarized as means ± SE. Statistical analyses were performed with SigmaStat (Jandel Scientific Software, San Rafael, CA) using paired or unpaired *t*-tests where appropriate. A p value < 0.05 was considered significant. All experiments were carried out at room temperature.

RESULTS

Activation of amiloride-insensitive chloride current by forskolin and PGE_2

In agreement with the observations of others (Yanase and Handler, 1986; Perkins and Handler, 1981; Chalfant et al., 1993; Niisato and Marunaka, 1997), increases of intracellular cAMP lead to activation of chloride currents in A6 epithelia. As indicated in the strip chart recording of Fig. 2 *A*, we have observed characteristically, following treatment with either forskolin or PGE_2, that the I_{sc} increases abruptly within tens of seconds to peak or quasi-plateau values (Păunescu, 1999). After what appears to be a short delay, the I_{sc} increases markedly and relatively slowly to substantially elevated plateau values within 20 to 30 min that are sustained for several hours. Addition of amiloride to forskolin- or PGE_2-stimulated tissues at the ends of 2-h experiments (not shown) characteristically resulted in large inhibitions of the I_{sc}. Compared to untreated tissues where the steady-state amiloride-insensitive currents, I_{sc}^{amil}, normally average in the range of 0.1–0.3 $\mu A/cm^2$ (Păunescu et al., 1997, 2000b) and that averaged 0.16 ± 0.03 $\mu A/cm^2$ (n = 6) in the present series of experiments (Fig. 2, *B* and *C*), the I_{sc}^{amil} of forskolin and PGE_2-treated tissues averaged 1.91 ± 0.18 $\mu A/cm^2$ (n = 12) and 1.66 ± 0.09 $\mu A/cm^2$ (n = 11), respectively. Because the responses to forskolin, PGE_2, exogenous cAMP, and theophylline caused similar increases of the amiloride-insensitive short-circuit currents (Păunescu, 1999; Păunescu and Helman, 1998, 2000), PGE_2 was used exclusively in the experiments reported below.

When amiloride-blocked tissues were challenged with PGE_2 as indicated in Fig. 2, *B* and *C*, the amiloride-insensitive short-circuit currents increased abruptly within 30 to 40 s to peak values, followed by relaxation of the currents in <10 min to stable but elevated values that were sustained for the duration of observation (1 to 2 h). In the absence of PGE_2 furosemide was without effect on the amiloride-insensitive currents (Fig. 2 *C*). In PGE_2-stimulated tissues furosemide addition to the basolateral solution inhibited reversibly, but not completely, the amiloride-insensitive current (Fig. 2, *B* and *C*). Peak current values averaged 3.32 ± 0.17 $\mu A/cm^2$ (amiloride, n = 3) and 2.26 ± 0.23 $\mu A/cm^2$ (amiloride + furosemide, n = 3) at 37.9 ± 2.7 s (n = 6) following exposure of the tissues to PGE_2. The currents decayed thereafter with a time constant of 2.48 ± 0.14 min (n = 6) to plateau values that averaged 1.20 ± 0.11 $\mu A/cm^2$ (amiloride, n = 3) and 0.51 ± 0.12 $\mu A/cm^2$ (amiloride + furosemide, n = 3). After additional treatment of amiloride-blocked tissues with furosemide, the currents decreased to 0.38 ± 0.04 $\mu A/cm^2$ (n = 3) (Fig. 2 *B*).

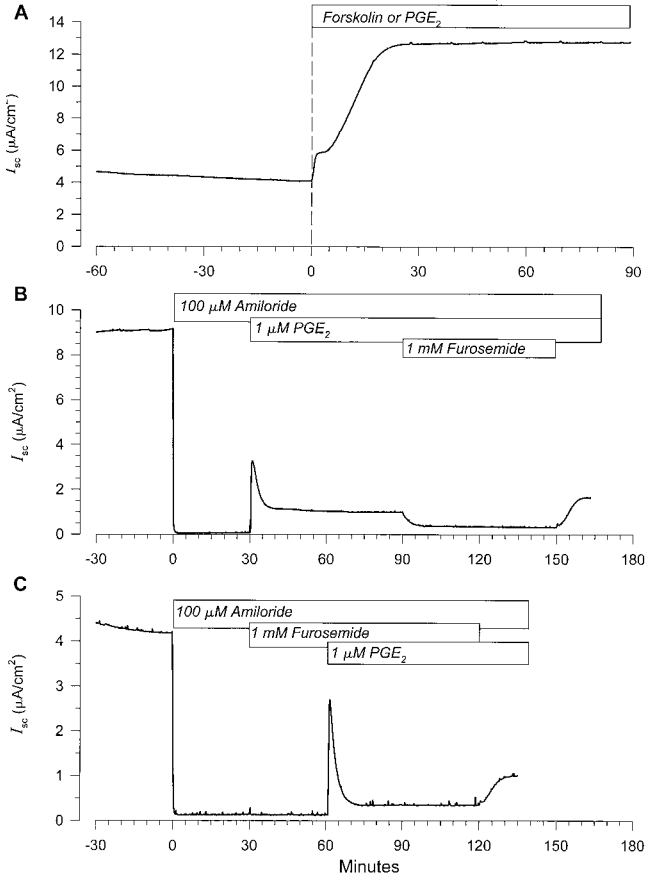

FIGURE 2 Typical strip chart recordings are shown of the short-circuit current responses to forskolin or PGE_2 in control (*A*) and amiloride-pretreated tissues (*B* and *C*). The tissue in *A* was treated with 25 μM forskolin.

Shown in expanded form in Fig. 3 are representative changes of I_{sc} (ΔI_{sc}) from basal levels caused by PGE_2 within 7 min in a control tissue, an amiloride-blocked tissue

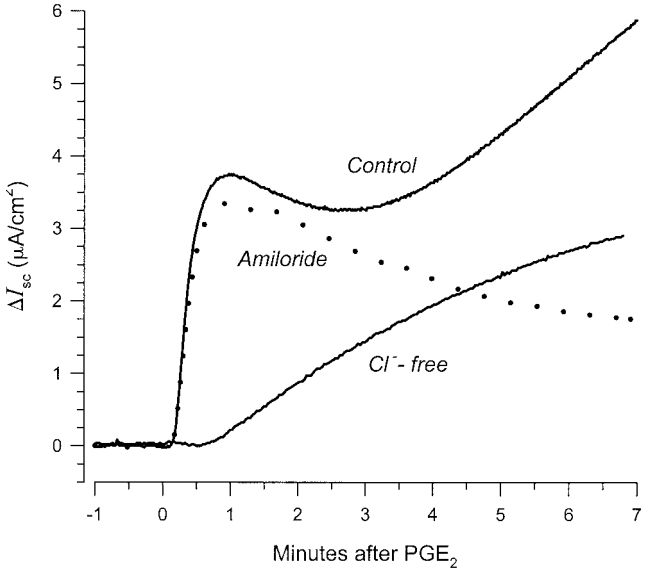

FIGURE 3 Time courses of change of the short-circuit current, ΔI_{sc}, caused by PGE_2 within the first 7 min in a control tissue and a tissue pretreated with amiloride that were bathed with the chloride-rich solution. Also shown is the time course of change of the ΔI_{sc} of a control tissue bathed with the chloride-free solution. The delay in onset of increase of the sodium current was ~30 s, at which time stimulation of chloride current was near maximal.

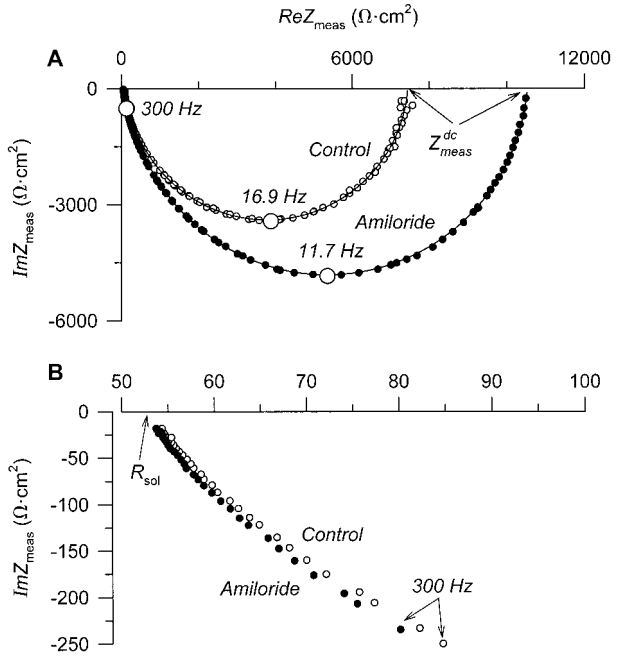

FIGURE 4 (*A*) Typical Nyquist plots of the measured impedance, Z_{meas}, are illustrated for a control tissue that was treated with amiloride. The frequencies of the impedance vectors are indicated at the apices of the semicircles and at 300 Hz. An expanded view of the impedance vectors between 300 Hz and 10,450 Hz is shown in *B*. The solid lines shown in *A* were determined by nonlinear curve-fitting of the impedance vectors to Eq. 1 (see text and Fig. 6).

bathed in the chloride-rich perfusion solution, and a control tissue bathed in chloride-free solution. Whereas currents in tissues with functional ENaCs exhibit relatively large secondary increases of amiloride-sensitive current (not shown), the delayed increases of current are absent in amiloride-pretreated tissues but are observed in chloride-free media. Notably, the abrupt increases of current are completely absent in chloride-free media, thereby providing evidence that the initial response to PGE_2 and forskolin is due to activation of a chloride conductance that precedes full activation of Na^+ transport. In these regards our observations are the same as those reported by Chalfant et al. (1993).

The amiloride-insensitive currents following PGE_2 or forskolin represent the maximal increases of chloride current at their peak and during the subsequent steady states of transport. In this regard it is relevant to note that the amiloride-insensitive basal short-circuit currents prior to PGE_2/forskolin are due principally to amiloride-insensitive Na^+ currents (Baxendale-Cox et al., 1997). It is unknown to what extent PGE_2/forskolin may activate amiloride-insensitive Na^+ current together with the chloride current. Consequently, the specific current due to chloride would be less than that measured by I_{sc}^{amil} if amiloride-insensitive Na^+ currents are increased by PGE_2/forskolin. Thus, for tissues continuously short-circuited, the steady-state chloride currents activated by PGE_2/forskolin are rather small in magnitude, averaging at most <2 $\mu A/cm^2$ in amiloride-blocked tissues and at most near 0.44 $\mu A/cm^2$ when tissues are additionally treated with furosemide. Neglecting the contribution of amiloride-insensitive Na^+ currents to the I_{sc}^{amil} of furosemide-treated tissues, furosemide inhibited between ~70–100% of the chloride current activated by PGE_2. If the I_{sc}^{amil} of PGE_2-treated tissues bathed in chloride-free solution is taken as an estimate of the amiloride-insensitive Na^+ current (0.47 ± 0.08 $\mu A/cm^2$, $n = 5$) then furosemide inhibited nearly 100% of the steady-state PGE_2-activated chloride current. In the absence of step changes of I_{sc}^{amil} in response to a high concentration of basolateral furosemide, it would be reasonable to conclude that furosemide acts to inhibit basolateral membrane chloride entry into the cells via an electroneutral mechanism(s) of transport because step changes of transcellular resistance, if they occurred, would cause step changes of short-circuit current that were never observed.

Impedance of control and amiloride-treated tissues

Typical Nyquist plots of the measured impedance (Z_{meas}) of control, unstimulated tissues before and after treatment with amiloride are illustrated in Fig. 4. I_{sc} averaged 7.41 ± 0.60 $\mu A/cm^2$ and was decreased to 0.46 ± 0.06 $\mu A/cm^2$ within 6 min after amiloride (Table 1). The impedance locus (Fig. 4 *A*) conformed to a depressed semicircle at frequencies

TABLE 1 Effect of 100 μM amiloride on the basal electrical parameters of short-circuited A6 epithelia

	I_{sc} (μA/cm^2)	R_T (k$\Omega \cdot$ cm^2)	R_p (k$\Omega \cdot$ cm^2)	R_{cell} (k$\Omega \cdot$ cm^2)	C_{eq}^{fit} (μF/cm^2)	f^{fit} (Hz)	γ^{fit}
Control	7.41 ± 0.60	6.11 ± 0.77	10.74 ± 1.83	15.83 ± 1.73	1.36 ± 0.04	21.7 ± 3.4	0.96 ± 0.012
6 min after Amiloride	0.46 ± 0.06	10.61 ± 1.81	—	262 ± 29	1.39 ± 0.04	13.5 ± 3.1	0.96 ± 0.003
45 min after Amiloride	0.27 ± 0.01	9.76 ± 1.58	10.03 ± 1.65	419 ± 22	1.40 ± 0.03	14.2 ± 3.1	0.96 ± 0.003

Values are means ± SE ($n = 6$) and where applicable are normalized to planar surface area. R_p were calculated by the method of Yonath and Civan (1971).

$<\sim$100 Hz and could be fit to an equation in the form of Eq. 1, thereby permitting estimation of the *dc* resistance. Although not apparent when viewed this way, the data points at frequencies >100 Hz did not conform to this equation (see below) and so the apparent resistance of apical and basolateral solutions, R_{sol}^{app}, calculated this way (156.6 ± 36.7 $\Omega \cdot$ cm^2, $n = 6$) overestimated the actual series resistance R_{sol} (47.5 ± 1.5 $\Omega \cdot$ cm^2, $n = 6$). The R_{sol} could be estimated by eye to within $\sim$1–2 $\Omega \cdot$ cm^2 by extrapolation of the ImZ_{meas} to the real axis. In practice, R_{sol} was determined by nonlinear curve-fitting of the ReZ_{meas} to infinite frequency using TableCurve (SPSS Inc., Chicago, IL). The transepithelial resistance (R_T) was determined as the difference between the *dc* value of Z_{meas} (Z_{meas}^{dc}) and the R_{sol}.

$$Z_{meas} = \frac{R^{fit}}{1 + (j\omega R^{fit} C_{eq}^{fit})^{\gamma^{fit}}} + R_{sol}^{app} \quad (1)$$

In these and all subsequent experiments, R_{sol} was not changed by amiloride nor PGE_2. Control R_T averaged 6.11 ± 0.77 k$\Omega \cdot$ cm^2 and at 6 and 45 min was increased to means of 10.61 and 9.76 k$\Omega \cdot$ cm^2, respectively, at these time points (Table 1). With the values of transepithelial conductance ($G_T = R_T^{-1}$) and short-circuit currents before and after amiloride, the shunt resistance $R_p = G_p^{-1}$ and the Thévenin emf of the cellular pathway for Na^+ transport (E_{Na}) were calculated using the method of Yonath and Civan (1971) where $G_T = I_{sc}/E_{Na} + G_p$. R_p averaged 10.74 and 10.03 k$\Omega \cdot$ cm^2 at 6 and 45 min after amiloride (Table 1) and the E_{Na} averaged 112.5 ± 4.3 mV ($n = 6$), which is quite typical for A6 and other tight epithelial tissues that transport Na^+ exclusively through apical membrane ENaCs (Helman and Liu, 1997; Koeppen et al., 1980; Helman and Thompson, 1982; Macchia and Helman, 1979; Yonath and Civan, 1971).

From the differences between R_T and R_p, the series resistance of apical and basolateral plasma membranes of the cells, $R_{cell} = R_a + R_b$, was calculated to have been increased by amiloride from 15.83 k$\Omega \cdot$ cm^2 to >260 k$\Omega \cdot$ cm^2 (Table 1). To the extent that control tissues express amiloride-sensitive ENaCs and amiloride-insensitive Na^+ currents that are small, the amiloride-insensitive resistance of the apical membrane is expected to be in the range of 250 k$\Omega \cdot$ cm^2 if apical membrane voltage is 100 mV and the blocker-insensitive Na^+ current, I_{sc}^{bi}, is 0.4 μA/cm^2. Thus, in control tissues, apical membranes are predominantly permeable to Na^+. If a finite apical membrane chloride conductance exists in control tissues, its value must be extremely low and immeasurably small.

Capacitance of control and amiloride-treated tissues

Frequency-dependent capacitances can arise from Maxwell-Wagner and/or Cole-Cole dielectric dispersions (Păunescu and Helman, 2001). At sufficiently high frequencies where the apical and basolateral membrane capacitive reactances are considerably less in value than their respective membrane resistances, the equivalent cell capacitance, $C_{eq} = C_a C_b/(C_a + C_b)$, would be constant if the C_a and C_b were frequency-independent. If, however, the capacitances exhibit audio frequency α-dispersions, C_{eq} would appear as a complex frequency-dependent capacitance C_{eq}^*.

At all frequencies $C_{eq}^* \equiv [j\omega(Z_a + Z_b)]^{-1}$ (Păunescu and Helman, 2001). Accordingly, the transepithelial impedance is given by Eq. 2 and C_{eq}^* can be determined from the measured values of Z_T and R_p. Shown in Fig. 5 *A* are typical results for a tissue in its control and amiloride-treated states. With increasing frequency, $|C_{eq}^*|$ decreased from values near 1.5 μF/cm^2 to near 0.9 μF/cm^2 at 10.45 kHz. Amiloride did not change the $|C_{eq}^*|$.

$$Z_T = \frac{R_p}{1 + j\omega R_p C_{eq}^*} \quad (2)$$

The mean $|C_{eq}^*|$ of amiloride-treated tissues is summarized in Fig. 5 *C*. The solid line fitted manually defines an approximate Cole-Cole α-dispersion with a characteristic frequency near 150 Hz. The deviations of $|C_{eq}^*|$ and phase angle ϕ of C_{eq}^* from pure Cole-Cole behavior shown by the manually fitted lines in Fig. 5, *C* and *D* at frequencies $<\sim$10 Hz are expected due to the Maxwell-Wagner-like dispersion (Păunescu and Helman, 2001). It should be stressed that manual fitting of a single Cole-Cole relaxation process to the data is not exact, and so the solid lines shown in Fig. 5, *B* and *C* should be taken as reasonable but imperfect approximations.

Shown also in Fig. 5 *B* are typical Nyquist plots of C_{eq}^* for the control and amiloride-treated states of the tissues. Significant deviations from single ideal depressed semicircles were observed, as expected at the lower frequencies corresponding to those associated with the Maxwell-Wagner dispersions (Păunescu and Helman, 2001).

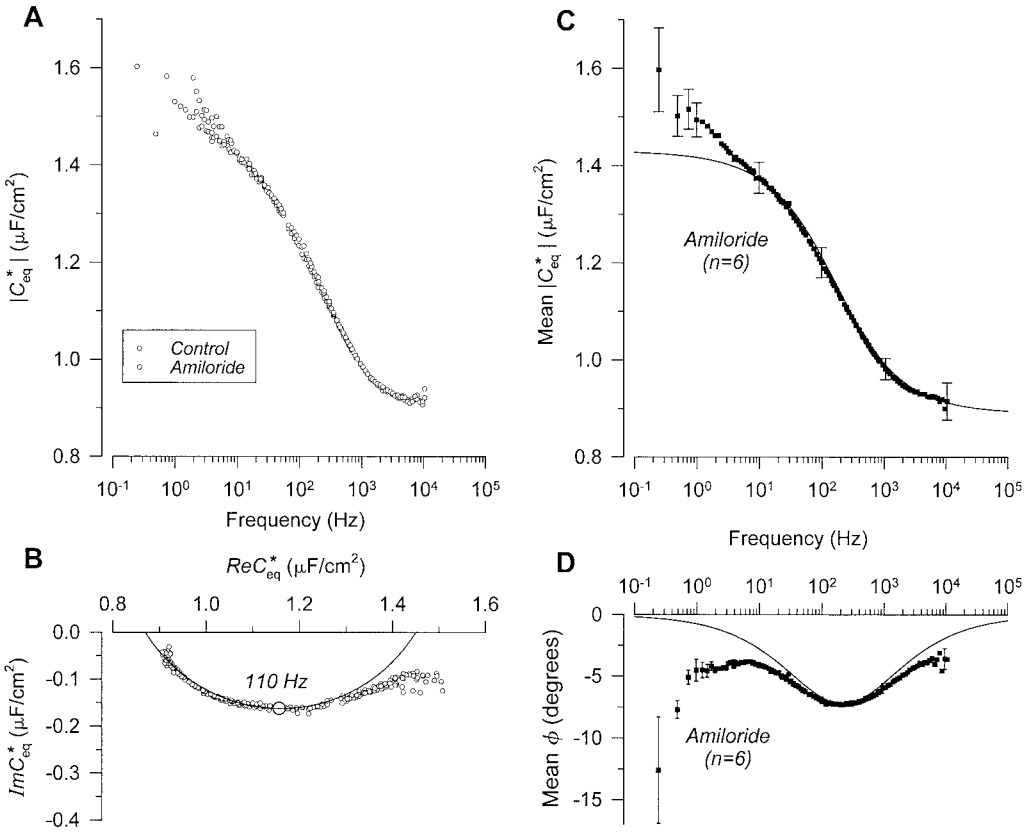

FIGURE 5 Apical membrane capacitance is frequency-dependent. Shown in *A* are typical plots of the dependence on frequency of the absolute values of the equivalent cell capacitance, $|C^*_{eq}|$, in the control state of a tissue and after inhibition of Na^+ transport by amiloride. When these data are plotted as Nyquist plots as indicated in *B*, the capacitance vectors appear to conform to a depressed semicircle (dielectric increment $\approx 0.58\ \mu F/cm^2$; Cole-Cole power law coefficient ≈ 0.65; characteristic frequency ≈ 110 Hz) at the higher frequencies. Significant deviations from a pure depressed semicircle at the lower frequencies are expected and observed due to the Maxwell-Wagner effect at the lower frequencies (Păunescu and Helman, 2001). A summary of the mean $|C^*_{eq}|$ is shown in *C* with selected standard error bars at the lower frequencies and at several higher frequencies for the purpose of clarity. The corresponding mean phase angles of C^*_{eq} are summarized in *D*. To illustrate the approximate contribution and location of the Cole-Cole relaxation process in *C* and *D* (*solid lines*), the parameters of the process were adjusted manually (dielectric increment = $0.54\ \mu F/cm^2$; power law coefficient = 0.625; characteristic frequency = 150 Hz; limiting static capacitance = $0.89\ \mu F/cm^2$) according to Eq. 5 in Păunescu and Helman (2001) to obtain an approximate fit of the lines to the mean data points. More robust methods were not attempted due to the less than adequate number and reliability of data points at the lowest frequencies.

Nevertheless, it was apparent, at least to a first approximation, that an α-relaxation process was responsible for the frequency dependence of C^*_{eq}. Because $C_a \ll C_b$ (see below), it follows that this dispersion arises predominantly from the apical membranes of the cells. Consequently, apical membrane capacitance could not be assumed to be constant in the audio range of frequencies.

Provided that the bandwidth of impedance vectors was limited to a maximum of ~50 Hz or less for the present set of experiments, it was possible to obtain satisfactory fits of the impedance vectors in this limited range of frequencies to Eq. 1, which is an equation of a depressed semicircle. Typically, as illustrated in Fig. 6 and viewed as Nyquist (Fig. 6, *A* and *B*) or Bode (Fig. 6, *C* and *D*) plots, the fitted lines deviated significantly from symmetrical depressed semicircles at frequencies >100 Hz. R^{app}_{sol} significantly underestimated the values of R_{sol} as noted above (Fig. 6 *B*).

Capacitance calculated at the apex of the fitted semicircle yielded mean values near 1.36 and 1.40 $\mu F/cm^2$ for control and amiloride-treated tissues, respectively (Table 1) at mean frequencies near 22 and 14 Hz, respectively. The corresponding mean values of $|C^*_{eq}|$ at these frequencies reported in Fig. 5 *C* are 1.33 ± 0.03 and $1.36 \pm 0.03\ \mu F/cm^2$ at 22 and 14 Hz, respectively, and are quite similar to the fitted values expected at these frequencies (Păunescu and Helman, 2001). It should be noted that the capacitances calculated at the apices of the fitted depressed semicircles are not unique, but will depend not only on the frequency dependence of C^*_{eq} but also on the values of $R^{fit} \approx R_p$ because the frequency at the apices $f^{fit} = (2\pi R^{fit}|C^*_{eq}|)^{-1}$. Consequently, differences in the tightness or leakiness of the paracellular shunt pathways will result in differences in f^{fit} and thus differences in capacitance calculated this way, even though C^*_{eq} has not changed.

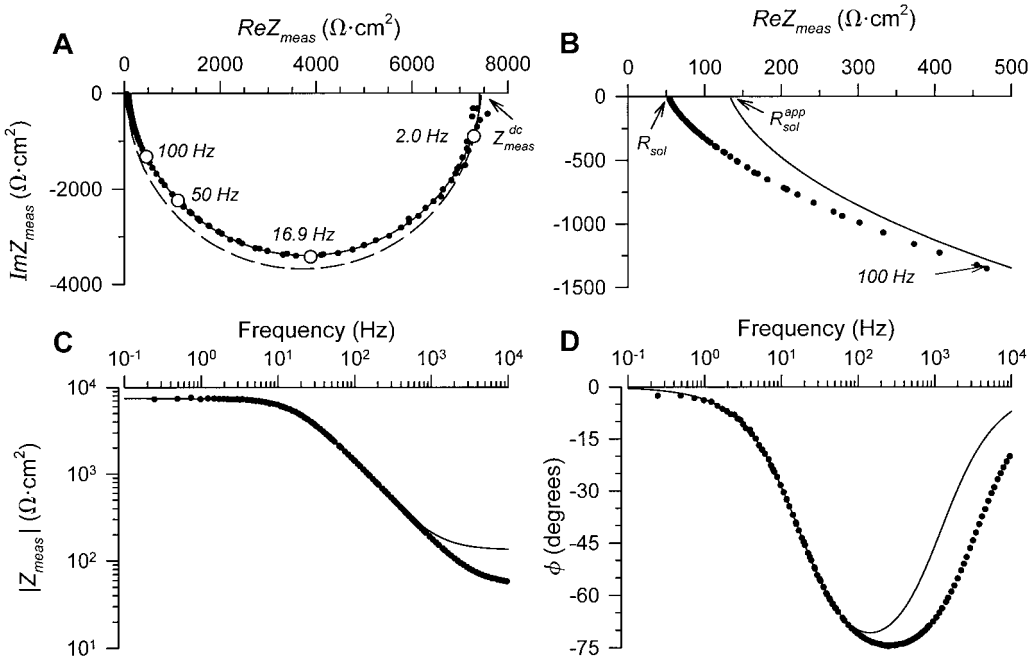

FIGURE 6 Impedance data of control and amiloride-treated tissues were fit to Eq. 1 at frequencies <50 Hz as shown by the solid lines in Nyquist (*A* and *B*) and Bode plots (*C* and *D*). (*A*) The fitted solid lines were depressed from ideal semicircles (*dashed line*). (*B*) Expanded view of *A* at higher frequencies. The solid fitted line deviated from the data points at frequencies >50 Hz and intersected the real axis at values of R_{sol}^{app} significantly less than those of R_{sol}, indicating that the impedance locus is skewed toward low frequencies.

PGE_2 activates a large apical membrane conductance to chloride

PGE_2 causes not only a dramatic decrease in transepithelial impedance but also a marked change of the impedance locus as indicated for a typical experiment, illustrated in Fig. 7. The change of impedance was clearly maximal at 2 min (not shown) at frequencies >5 Hz. The impedance at the very low frequencies <~3–4 Hz could not be resolved during the transient relaxation of currents that violated the requirement of steady-state currents and voltages to measure impedance. It should be noted that these experiments were carried out in the presence of amiloride to block Na^+ currents so that the responses could be attributed to an increase of Cl^- conductance. R_T of the amiloride-treated tissue in Fig. 7 was decreased from near 13 to 4 $k\Omega \cdot cm^2$. From control values of 0.27 ± 0.01 $\mu A/cm^2$, the I_{sc}^{amil} averaged at 16 and 45 min after PGE_2 2.01 and 1.93 $\mu A/cm^2$, respectively. The mean R_T was decreased from amiloride control values near 10 $k\Omega \cdot cm^2$ (Table 1) to 3.52 and 3.39 $k\Omega \cdot cm^2$ (Table 2), respectively, at these same time points. Within 2 min PGE_2 caused maximal decreases of impedance that were sustained. The changes of impedance were reversible after withdrawal of PGE_2 although reversal was considerably slower (Fig. 7 *C*) and not quite complete at 45 min. From the PGE_2-stimulated I_{sc}^{amil} of 1.82 ± 0.07 $\mu A/cm^2$ ($n = 6$), the I_{sc}^{amil} decreased after PGE_2 washout at 2, 6, and 45 min to 1.02 ± 0.07, 0.74 ± 0.06, and 0.39 ± 0.03 $\mu A/cm^2$, respectively.

The impedance vectors normalized to the values of Z_{meas}^{dc} (Fig. 7 *B*) more clearly indicate that the impedance locus was changed by PGE_2 from a single depressed semicircle at frequencies <50 Hz in the amiloride control state to a locus consistent with a large decrease of apical membrane resistance. Under these latter circumstances where apical membrane resistance, R_a, is decreased by PGE_2 into a range of values comparable in magnitude to the basolateral membrane resistance, R_b, and where in addition the time constants of apical and basolateral membranes are sufficiently different from each other to result in observable interacting semicircles in Nyquist plots, the measured impedance is quite generally:

$$Z_{meas} = \frac{(Z_a + Z_b)R_p}{Z_a + Z_b + R_p} + R_{sol} \quad (3)$$

where apical (Z_a) and basolateral (Z_b) membrane impedances are:

$$Z_a = \frac{R_a^{fit}}{1 + (j\omega R_a^{fit} C_a^{fit})^{\gamma_a^{fit}}} \quad (4)$$

$$Z_b = \frac{R_b^{fit}}{1 + (j\omega R_b^{fit} C_b^{fit})^{\gamma_b^{fit}}} \quad (5)$$

It should be emphasized here, as above, that the values of C_a^{fit} and C_b^{fit} are those at the unique frequencies at the apices of the semicircles and where the semicircles would be

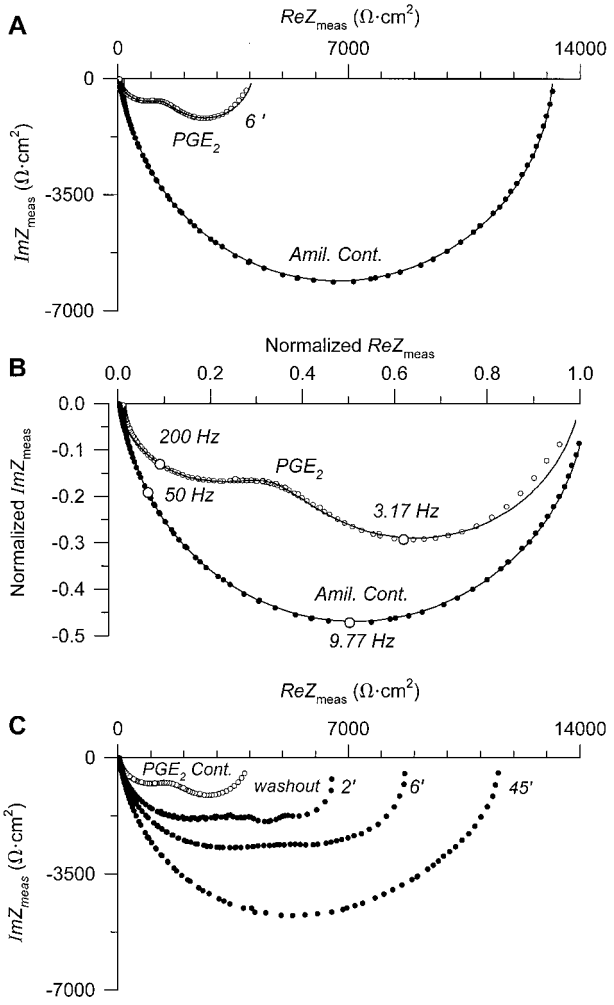

FIGURE 7 PGE_2 causes a dramatic change of impedance and its locus, as indicated in *A*. The data of *A* were normalized to the values of Z^{dc}_{meas} to better illustrate the change of impedance locus as shown in *B*. The impedance vectors at the lower frequencies $<\sim$200 Hz of PGE_2-treated tissues required the fitting of at least two depressed semicircles (*solid line*) to Eq. 3 (see text). The effects of PGE_2 were partially reversible within 45 min, as indicated in *C*. In comparison with the onset of PGE_2 effects on impedance the washout was relatively slow, as indicated by the changes of impedance locus at 2, 6, and 45 min.

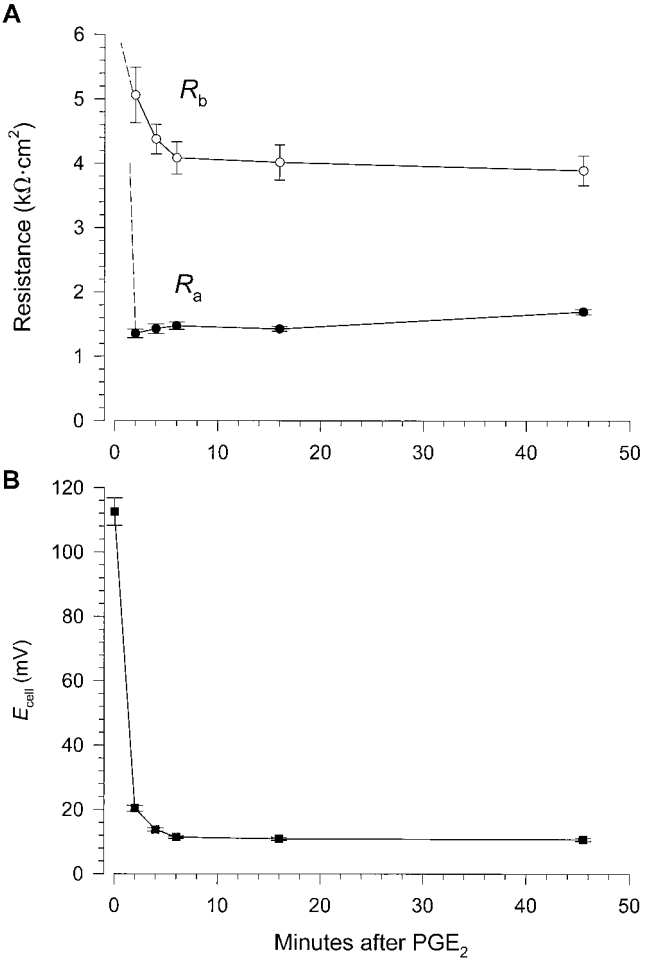

FIGURE 8 PGE_2 causes decrease of both apical (R_a) and basolateral membrane (R_b) resistance of amiloride-pretreated tissues as shown in *A*. Whereas the decrease of R_a is maximal within 2 min, the decrease of R_b is relatively slow, but essentially complete within $\sim$6–10 min. The corresponding changes of the transcellular Thévenin emf, E_{cell}, are shown in *B* (see text).

depressed if the power law dependencies γ_a^{fit} and γ_b^{fit} were less than unity due to capacitance being frequency-dependent (Păunescu and Helman, 2001).

To determine apical and basolateral membrane resistances and capacitances, impedance data were fit by nonlinear curve-fitting (Scientist for Windows, MicroMath, Inc., Salt Lake City, UT) to Eq. 3 at frequencies $<$50 Hz for the amiloride control data, as was indicated above, and at frequencies $<$200 Hz when tissues were treated with PGE_2 (Fig. 7). Starting values of R_p were determined independently before treatment of the tissues with PGE_2. Starting values of R_a and R_b were estimated with the values of R_{cell} and the fractional transcellular resistances ($R_a/(R_a + R_b)$) that were evident by inspection of the impedance plots. C_a and C_b were estimated at frequencies corresponding to the approximate apices of the impedance loci. We will refer to the apical and basolateral membrane resistances and capacitances below simply as R_a, R_b, C_a, and C_b, recognizing that these parameters were determined by fitting of the impedance loci to Eq. 3 at the very low audio frequencies.

During steady-state periods of transport and at time points of 16 and 45 min, R_a averaged 1.42 and 1.70 k$\Omega \cdot cm^2$ and R_b averaged 4.02 and 3.90 k$\Omega \cdot cm^2$, respectively (Table 2). R_p averaged near 10 k$\Omega \cdot cm^2$ (Table 2) and was essentially unchanged by PGE_2. Although it was not possible to determine the values of R_b before PGE_2 in control or amiloride-blocked tissues, the PGE_2-related time-dependent changes of R_a and R_b could be assessed as indicated in Fig. 8 *A*. R_a was maximally decreased from greater than a few hundred k$\Omega \cdot cm^2$ within 2 min by PGE_2 and remained

essentially constant for the 45 min period of observation. In contrast, it became apparent following PGE_2 that R_b decreased from >5 k$\Omega \cdot cm^2$ to steady-state values near 4.0 k$\Omega \cdot cm^2$ within 6 min. R_b in control tissues determined by a different method was found to average >6.6 k$\Omega \cdot cm^2$ (Păunescu, 1999) and 9.0 k$\Omega \cdot cm^2$ (Păunescu et al., 2000b), which would be consistent with the time-dependent decrease of R_b measured here by impedance of tissues treated with PGE_2. Accordingly, whereas the PGE_2-related decrease of R_b was relatively small and relatively slow, the major and very rapid effect of PGE_2 was to decrease the apical membrane resistance to values considerably less than those of the basolateral membranes of the cells.

Transcellular emfs

The magnitudes of the transcellular current before and after PGE_2 will be determined not only by R_a and R_b, but also by changes of the transcellular driving force E_{cell} where $E_{cell} = E_a + E_b$ and where E_a and E_b are, respectively, the Thévenin emfs of apical and basolateral membranes. Accordingly, $I_{sc} = (E_a + E_b)/(R_a + R_b) = E_{cell}/(R_a + R_b)$. Before PGE_2, where apical membranes are populated principally if not solely by amiloride-sensitive and -insensitive Na^+ channels and where E_a is at or very near zero (Păunescu and Helman, 2001), $I_{sc} = E_b/(R_a + R_b)$. If the R_b is determined principally by the conductance of basolateral membrane K^+ channels, then at zero current flow through the basolateral membrane, $E_b = |\mathcal{E}_K + I_{pump}R_b|$ (Helman and Thompson, 1982), where $\mathcal{E}_K$ is the Nernst equilibrium potential difference and I_{pump} is the current generated by the Na,K-ATPase. Accordingly, relatively fast decreases of R_b that occur before appreciable changes of $\mathcal{E}_K$ or I_{pump} would be expected to cause increases of E_b, which together with decreases of R_b would lead to stimulation of I_{sc}. Although decreases of R_b will lead to increases of I_{sc}, E_{cell} would be expected to increase if the channels expressed at apical membranes were exclusively Na^+ channels, as would be the case for tight epithelia like frog skin and toad urinary bladder, where generally $E_{cell} = E_{Na}$ averages above 100 mV and as indicated above, 112.5 mV for the A6 epithelia of the present experiments.

For tissues like A6, where cAMP activates both Na^+ and Cl^- channels and where chloride channels are relatively close to electrochemical equilibrium, the E_a after PGE_2 must move toward the Nernst equilibrium potential difference of Cl^-, $\mathcal{E}_{Cl}$. With amiloride-blocked tissues where apical membranes express blocker-insensitive Na^+ channels (R^{bi}_{Na}), $E_a = (E_{Cl}R^{bi}_{Na})/(R^{bi}_{Na} + R_{Cl})$. Because $R_{Cl} \ll R^{bi}_{Na}$, after PGE_2 E_a can practically be equated with $\mathcal{E}_{Cl}$. Thus, with reference to a grounded apical solution, $E_{cell} = E_b - \mathcal{E}_{Cl} = I^{amil}_{sc}(R_a + R_b)$ so that E_{cell} can be calculated from the I^{amil}_{sc} and transcellular slope resistance ($R_a + R_b$). As indicated in Fig. 8 *B*, E_{cell} decreased dramatically within 2 min from 112.5 mV to mean values of 20.4 mV, and then to 10.9 and 10.7 mV at 16 and 45 min, respectively, after PGE_2. Consequently, despite a rapid opening of a large apical membrane Cl^- conductance within 2 min, the initial peak magnitude of the chloride current ($I_{Cl} = (V_a - \mathcal{E}_{Cl})/R_{Cl}$) was compensated for by a correspondingly large decrease of E_{cell}. Because Cl^- current enters the cells initially, $V_a > \mathcal{E}_{Cl}$. With loss of Cl^- from the cells and increase of $\mathcal{E}_{Cl}$, E_{cell} declines toward steady-state values, as does the $V_a - \mathcal{E}_{Cl}$ and hence the Cl^- current component of I^{amil}_{sc}.

The apical membrane Na^+ current components of I^{amil}_{sc} during these times are $I^{bi}_{Na} = V_a/R^{bi}_{Na}$, so that $I^{amil}_{sc} = I^{bi}_{Na} + I_{Cl}$. Because $R^{bi}_{Na} \gg R_{Cl}$, the rapid initial increases of I^{amil}_{sc} must be due to I_{Cl}, with I_{Cl} relaxing to its steady-state value where chloride secretion is determined principally by the rate of basolateral membrane Cl^- entry (see Appendix). If the basolateral membrane chloride entry were zero, then chloride must come to electrochemical equilibrium at the apical membranes of the cells where at the steady state $I_{Cl} = 0$ or chloride secretion would be absent despite high values of apical membrane conductance to Cl^-.

TABLE 2 Electrical parameters of amiloride-pretreated A6 epithelia stimulated by PGE_2

	I^{amil}_{sc} (μA/cm^2)	R_T (k$\Omega \cdot$ cm^2)	R_p (k$\Omega \cdot$ cm^2)	R^{fit}_a (k$\Omega \cdot$ cm^2)	R^{fit}_b (k$\Omega \cdot$ cm^2)	R_{cell} (k$\Omega \cdot$ cm^2)
16 min after PGE_2	2.01 ± 0.09	3.52 ± 0.34	10.53 ± 1.64	1.42 ± 0.04	4.02 ± 0.27	5.45 ± 0.26
45 min after PGE_2	1.93 ± 0.11	3.39 ± 0.36	9.32 ± 1.66	1.70 ± 0.04	3.90 ± 0.24	5.59 ± 0.24

	C^{fit}_a (μF/cm^2)	C^{fit}_b (μF/cm^2)	C^{fit}_{eq} (μF/cm^2)	f^{fit}_a (Hz)	f^{fit}_b (Hz)	γ^{fit}_a	γ^{fit}_b
16 min after PGE_2	1.38 ± 0.03	20.1 ± 0.7	1.29 ± 0.03	81.2 ± 2.1	2.0 ± 0.12	0.85 ± 0.003	0.89 ± 0.008
45 min after PGE_2	1.39 ± 0.03	20.2 ± 0.8	1.30 ± 0.03	67.6 ± 0.7	2.1 ± 0.10	0.86 ± 0.004	0.92 ± 0.005

Values are means ± SE ($n = 5$) and where applicable are normalized to planar surface area.

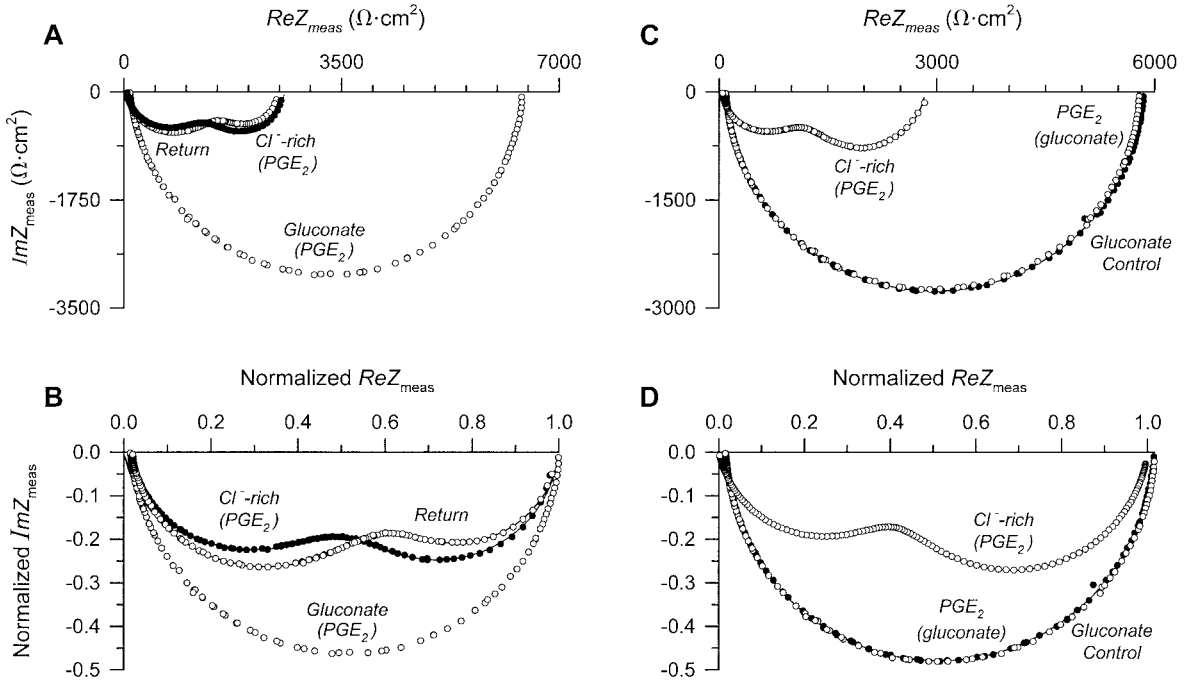

FIGURE 9 The changes of impedance and its locus caused by PGE_2 are dependent on chloride. In *A*, gluconate replaced all chloride in the apical and basolateral solutions bathing a tissue that had already been treated with PGE_2 and amiloride. The effect of chloride removal was completely reversible upon return to the chloride-rich solution. The impedance vectors in *A* normalized to the values of Z^{dc}_{meas} are shown in *B*. In *C* the tissue was treated with PGE_2 while it was bathed with the chloride-free gluconate solution, causing a minuscule change of impedance. Exposure to the chloride-rich solution caused a typical change of impedance and its locus. The normalized impedance vectors in *C* are shown in *D*.

Depressed semicircles of impedance loci

Because capacitance is frequency-dependent, it is expected that the impedance locus would consist of depressed semicircles (Păunescu and Helman, 2001). Nonlinear curve-fitting of the impedance vectors as indicated above yielded mean power law dependencies γ_a and γ_b near 0.85 and 0.90, respectively (Table 2). The absolute values of capacitance at the apices of the depressed semicircles $|C_a|$ and $|C_b|$ averaged near 1.38 and 20.1 $\mu F/cm^2$, respectively, in PGE_2-treated tissues. The frequencies at the apices averaged ~70–80 Hz for $|C_a|$ and ~2.0 Hz for $|C_b|$ (Table 2).

PGE_2-related changes of impedance in amiloride–blocked tissues require Cl^-

To ensure that PGE_2 activated a chloride conductance in the tissues we studied, two experimental protocols were used to test for chloride dependence of the PGE_2-related changes of impedance in amiloride-pretreated tissues. In experiments illustrated in Fig. 9, *A* and *B*, tissues bathed in chloride-rich solution were treated first with PGE_2 and then exposed to a chloride-free gluconate solution. In the experiments illustrated in Fig. 9, *C* and *D*, tissues were bathed first with chloride-free solution, treated with PGE_2 in the absence of chloride, and then exposed to a chloride-rich solution. Regardless of the sequence, removal of chloride in the PGE_2-treated states of the tissues caused reversible decreases of the I_{sc}^{amil} to 0.47 ± 0.08 $\mu A/cm^2$ from 1.75 ± 0.08 $\mu A/cm^2$ ($n = 5$). The R_T and impedance locus were unchanged by PGE_2 when tissues were bathed in chloride-free solution (Fig. 9 *C*). Subsequent exposure to the chloride-rich solution resulted in a decrease of R_T and a change of the impedance locus (Fig. 9, *C* and *D*). Removal of chloride from tissues treated first with PGE_2 resulted in reversible increases of R_T and changes of the impedance locus (Fig. 9 *A*). These specific chloride-dependent changes of current, resistance, and impedance locus provide compelling evidence to support the view that PGE_2 acting through cAMP activates a large chloride conductance at the apical membranes of the cells that precedes significant activation of apical membrane ENaCs, and hence the amiloride-sensitive apical membrane Na^+ conductance. Thus, the R_a of amiloride- and PGE_2-treated tissues can be equated with the apical membrane resistance to chloride, R_{Cl}. To the extent that in control tissues PGE_2 stimulates Na^+ transport about threefold (Păunescu and Helman, 1997; Păunescu, 1999) to ~20 $\mu A/cm^2$, the amiloride-sensitive Na^+ resistance, R^{bs}_{Na}, would be ~5.6 $k\Omega \cdot cm^2$ (112.5 mV/20 $\mu A/cm^2$) or about three to fourfold larger than R_{Cl} in PGE_2-treated A6 epithelia.

Time-dependent change of capacitance

In the face of a frequency-dependent apical membrane capacitance and changes of resistance, we could not rely on

the estimates of capacitance at the apices of the semicircles to evaluate changes of capacitance caused by PGE_2 because it was not possible to compare the capacitances at the same frequencies in control and PGE_2-stimulated states of the tissues. Instead, we evaluated the changes of $|C^*_{eq}|$ caused by PGE_2 where we could compare capacitance at all frequencies. We were particularly interested in evaluating the data at the higher frequencies, because at sufficiently high frequencies the apical membrane capacitive reactance, $X_a = (j\omega C^*_a)^{-1}$, decreases to values substantially less than those of the apical membrane resistance so that the Z_a can be equated with X_a. Because of the relatively high basolateral membrane capacitance and resistance, it is readily appreciated that at high frequencies the basolateral membrane impedance can be equated with its capacitive reactance. Although we do not know the frequency dependence of C^*_b, its contribution to C^*_{eq} at the higher frequencies would be relatively small if the ratio of C_b/C_a near 15:1 (Table 2) at the lower frequencies is indicative of its ratio at higher frequencies. Accordingly, $|C^*_{eq}|$ approaches values near the apical membrane capacitance $|C^*_a|$ when $X_a \ll R_a$.

Shown in Fig. 10 *A* for a representative experiment are the $|C^*_{eq}|$ at frequencies between 250 Hz and 10 kHz in the control state of the tissue and at various time points between 2 and 45 min after treating the tissue with PGE_2. It was evident that PGE_2 caused an increase of $|C^*_{eq}|$ at every frequency and at every time point. It was also evident at frequencies >1000 Hz that capacitance increased relatively slowly with small increases discernible at 2 min but with the dominant increase occurring between 2 min and 16 min. Bearing in mind that PGE_2 decreases apical membrane resistance to values near 1.5 $k\Omega \cdot cm^2$ and that this analysis requires that $X_a \ll R_a$, we assumed as a criterion that this condition was met when at sufficiently high frequencies values of $|C^*_{eq}|$ normalized to their control values were constant (independent of frequency). Typically, as determined empirically, this criterion was satisfied at frequencies >~1500 Hz, as indicated in Fig. 10 *B* for time points of 2, 6, and 45 min. At frequencies above 8 kHz the uncertainties in difference of values between Z_{meas} and those of R_{sol} limited reliable evaluation of the normalized $|C^*_{eq}|$ as the difference values approached zero. To summarize, the normalized values of $|C^*_{eq}|$ were averaged between 1.5 and 4.0 kHz at each time point after PGE_2.

Shown in Fig. 10 *C* is a summary of the time-dependent changes of $|C^*_{eq}|$ caused by PGE_2. After a short delay of <1 min capacitance was increased at 45 min by 9.8 ± 0.3% ($n = 6$). The best fit line to the data points was determined by nonlinear curve-fitting using the set of transition functions in TableCurve (SPSS Inc., Chicago, IL). The data were best fit to a Weibull cumulative function. This line and other asymmetric transition functions that fit nearly as well (pulse cumulative with power term, log-normal cumulative) all indicated that the onset of response of capacitance to PGE_2 was delayed by ~1 min. For comparison of time course, the I^{amil}_{sc} response to PGE_2 shown in Fig. 2 *B* is reproduced in Fig. 10 *C*. Remarkably, capacitance increased relatively slowly toward a sustained plateau within ~20–30 min, paralleling the time-dependent increases of amiloride-sensitive short-circuit current attributable to stimulation of Na^+ transport and apical membrane functional ENaC densities (Helman and Păunescu, 1998; Păunescu and Helman, 1997; Păunescu, 1999; Els and Helman, 1997). These find-

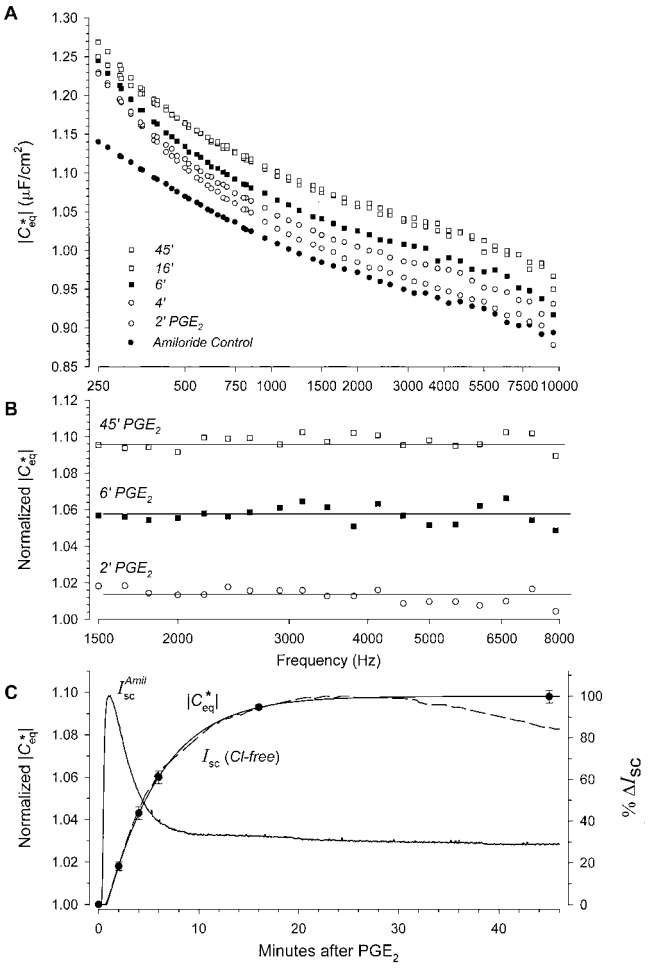

FIGURE 10 Shown in *A* are the absolute values of the equivalent cell capacitance, $|C^*_{eq}|$, at frequencies between 250 Hz and 10 kHz for a typical tissue in its amiloride control state and at the time intervals indicated following treatment with PGE_2. Shown in *B* are the values of $|C^*_{eq}|$ at 2, 6, and 45 min after PGE_2 normalized to their control values at the same frequencies between 1.5 and 8.0 kHz. Intermediate time points at 4 and 16 min have been omitted for clarity. Although the $|C^*_{eq}|$ are dependent on frequency, the normalized changes of $|C^*_{eq}|$ are constant (independent of frequency) in this range of frequencies. The mean of the 19 normalized values of $|C^*_{eq}|$ are indicated by the solid lines. A summary (means ± SE, $n = 6$) of the time-dependent increases of the normalized $|C^*_{eq}|$ is shown in *C*. Also shown in *C* for the purpose of direct comparison of time courses are typical normalized time-dependent changes of short-circuit current in a tissue pretreated with amiloride and bathed in chloride-rich solution (see Fig. 2 *B*), and a control tissue bathed with chloride-free gluconate Ringer's solution (*dashed line*) where basal and PGE_2-stimulated currents are amiloride-inhibitable.

ings are perhaps more remarkable given the rapidity (<1 min) with which PGE_2 maximally activates the apical membrane chloride conductance. Indeed, there is a virtually complete dissociation in time between activation of chloride and sodium conductances. In this regard the changes of capacitance caused by PGE_2 are correlated with activation of sodium conductance. If increases of capacitance are associated with activation of chloride conductance in A6 epithelia, they are undetectable by the methods used in our studies.

DISCUSSION

Chloride transport

Although PGE_2 is a potent activator of Na^+ transport in A6 epithelia (Kokko et al., 1994; Matsumoto et al., 1997; Păunescu and Helman, 1997), its effect on chloride transport is relatively minor. According to our own analysis, chloride transport is stimulated maximally by PGE_2 within 1 min and well before onset of appreciable increases of Na^+ transport. Furosemide reversibly inhibits the steady-state PGE_2-activated chloride transport, does not block the PGE_2 activation of apical membrane chloride conductance, and thus acts most likely through inhibition of Cl^- entry into the cells through an electroneutral transporter at the basolateral membranes of the cells (Fan et al., 1992; see Appendix).

In the absence of PGE_2 the apical membranes are permeable only to Na^+, principally through amiloride-sensitive ENaCs but also, to a relatively small degree, through amiloride-insensitive Na^+ channels (Baxendale-Cox et al., 1997; Helman et al., 1998). In this regard the impedance locus of control tissues, and in particular amiloride-blocked control tissues, behaved as though the fractional transcellular resistances approached values of unity, indicating that the apical membrane resistance was far greater in value than the basolateral membrane resistance. Consequently, apical membrane chloride conductance in the absence of PGE_2 is for all practical purposes at or near zero, so that chloride channels are either in a permanently shut state or have open probabilities very near zero.

Clearly, PGE_2/cAMP activation of chloride conductance is remarkably a very rapid process that in the A6 epithelia we studied causes a large decrease of apical membrane resistance to values that averaged near 1500 $\Omega \cdot cm^2$ in amiloride-blocked tissues. To achieve steady-state chloride currents at the apical membranes that averaged near 2 $\mu A/cm^2$, a small net electrochemical driving force of 3 mV displaced from equilibrium would be required. Such a rapid increase of chloride conductance requires direct activation of channels that are resident within the apical membranes and/or an equally rapid translocation of chloride channel-containing vesicles from the cytosol to the apical membranes of the cells (see below), where the channels are already functional or become functional within seconds once they have reached the apical membranes. Interestingly, Kokko et al. (1997) have noted that PGE_2 activates chloride channels in cell-attached patches, which is a procedure that completely prevents cAMP activation of ENaCs (Marunaka and Eaton, 1991). Because chloride channels are activated in cell-attached patches even though patch formation completely disrupts activation of ENaCs, the implication is that the activation process does not involve trafficking of new chloride channels to the apical membranes (Kokko et al., 1997) (see Capacitance below).

Functional channel densities

Patch clamp experiments have also revealed that PGE_2-activated apical membrane chloride channels in A6 epithelia are characterized by a single channel conductance of 7 pS and an open probability near 0.5 (Kokko et al., 1997). Hence, the apical membrane density of open chloride channels activated by PGE_2 is ~95 million channels/cm^2 (or 95 channels per cell = (10^6 cells/cm^2 × 1500 $\Omega \cdot cm^2$ × 7 pS/channel)$^{-1}$) and the total number of open and closed channels is therefore ~190 channels/cell that are maximally activated by PGE_2. Such calculations serve to point out under maximal conditions of channel activation that the densities of channels involved in transport are remarkably low. Hence, it becomes particularly important in assessing location and trafficking of chloride channels to use methods of detection with sufficient sensitivity that take into account the relatively few functional channels actually involved in changes of apical membrane chloride conductance and transport.

Capacitance

Changes of capacitance have been used widely as an index of change of membrane area. However, a complicating factor is the existence of audio frequency dispersions regardless of whether they arise from Maxwell-Wagner and/or Cole-Cole dielectric dispersions. Our results here, as elsewhere (Liu et al., 1995; Liu and Helman, 1998), clearly indicate that apical membranes of A6 epithelia exhibit a major dielectric dispersion at low audio frequencies with absolute values of capacitance decreasing from near 1.5 $\mu F/cm^2$ to near 0.9 $\mu F/cm^2$ as frequency nears 10 kHz. It should be emphasized that currents, resistances, and capacitances reported here have been normalized to the planar surface area of the tissue. Actual membrane areas of apical and basolateral membranes are not known. Although there is considerable uncertainty in knowing the actual apical membrane area, it is known from recent confocal microscopic studies that apical membranes of living cells of A6 epithelia are dome-shaped (Butterworth et al., 2001). Thus, actual apical membrane area may, as a rough approximation, be about twice the planar area so that capacitance

normalized to actual area is more likely in the vicinity of 0.45 (~10 kHz) to 0.75 $\mu F/cm^2$ (*dc*). To the extent that the capacitance of a vacuum with a dielectric thickness of 40–60 Å is in the range of 0.15–0.22 $\mu F/cm^2$ (Awayda et al., 1999), it is clear that dielectric increments that give rise to two to threefold increases of capacitance above vacuum must exist at radio and/or higher frequencies to account for the capacitance at 10 kHz. The major dielectric increment (0.9 to 1.5 $\mu F/cm^2$), however, exists at audio frequencies, where changes not only of area, but also changes of the α-dispersion dielectric increment and/or its relaxation frequency can give rise to changes of capacitance unrelated to changes of membrane area, and so confound interpretation of changes of capacitance. In this regard we chose, as have Van Driessche and his colleagues (Zeiske et al., 1998; Atia et al., 1999) to measure capacitance in the kHz range of frequencies where changes of capacitance, when they occurred, could be due to change of membrane area and/or change of dielectric increments at radio or higher frequencies. To the extent that it is impossible with intact epithelia to measure capacitances at these higher frequencies to verify constancy of the dielectric increments, it remains impossible to conclude unequivocally that changes of capacitance are due to changes of membrane area. Nevertheless, more recent observations have indicated parallel time-dependent changes of Na^+ transport rates, apical membrane ENaC densities, and vesicle endocytosis upon withdrawal of forskolin from pretreated A6 epithelia, suggesting that cAMP-dependent changes of channel densities occur by trafficking of channels to the apical membranes of the cells (Butterworth et al., 2001). Hence, it would be plausible to believe that the changes of capacitance observed in our experiments are related to changes of membrane area. Indeed, the time course of change of capacitance, together with its relatively delayed and slow onset and increase toward sustained plateau values within ~20–30 min, suggests that the observed increases of capacitance could be due mainly if not solely to vesicle trafficking of Na^+ channels to the apical membranes of the cells. In this regard it is especially noteworthy that capacitance was not changed within 1 min, at which time chloride conductance was increased maximally. On the one hand, this could be interpreted to indicate that PGE_2 activates chloride channels that are resident within the apical membranes. On the other hand, we do not know how many chloride channels can be packaged within a single vesicle. If the density of packaging of channels per vesicle is high, then it would remain possible that only a few chloride-containing vesicles are involved in exocytosis that could result in undetectable changes of membrane area/capacitance, thereby requiring that no firm conclusion be made regarding the origin of chloride channels activated by PGE_2/cAMP.

Our findings with regard to PGE_2-related increases of capacitance are quantitatively similar to those reported by Zeiske et al. (1998) and Atia et al. (1999) who reported that a variety of hormones/agents that increase intracellular cAMP cause about an 8% increase of capacitance measured at kHz frequencies in A6 epithelia bathed with an NaCl-free apical solution. Under these conditions the peak increases of capacitance were in some but not all cases delayed from the peak increases of the chloride short-circuit current and the transepithelial conductance. Accordingly, it was suggested that activation of chloride conductance might be explained by an increase of membrane area. Such a conclusion is, however, untenable under the conditions of our own experiments, where we observed unequivocally a marked time-dependent difference in activation of chloride and sodium currents that was virtually identical to that originally reported by Chalfant et al. (1993). Because the onset of the time-dependent increases of capacitances was clearly delayed from the peak maximal changes of chloride current and conductance, and the increases of capacitance we observed paralleled the much slower time-dependent increases of sodium current and apical membrane functional ENaC densities (Els and Helman, 1997; Păunescu and Helman, 1997; Helman and Păunescu, 1998; Păunescu, 1999), we conclude that the increases of capacitance are correlated with activation of Na^+ transport in A6 epithelia possibly by vesicle trafficking of channels to the apical membranes of the cells.

It remains of particular interest to know whether, and if so, how, removal of all apical solution NaCl and/or other factors may influence the time constants for activation of ENaC and chloride channel densities at the apical membranes of the cells, especially in view of recent observations that inhibition of an LY294002-inhibitable PI3-kinase(s) markedly prolongs the short-circuit current response of A6 epithelia to cAMP (Păunescu et al., 2000a). Notwithstanding the reason(s) for differences in the rates of activation of Na^+ and chloride conductance, the absence of detectable changes of capacitance associated with chloride conductance and the remarkable similarity in the time course of the increase of capacitance, Na^+ transport and functional ENaCs argue in favor of a cAMP-mediated mechanism that may involve vesicle trafficking of ENaCs to the apical membranes of the cells. Regardless of these time-dependent correlations of capacitance and transport, it will ultimately be necessary to know not only the actual changes of apical membrane area due to vesicle endocytosis and exocytosis, but also whether one or more populations of vesicles contain subunits of channels and/or functional chloride channels and ENaCs that are trafficked to the apical membranes of the cells.

APPENDIX

Estimates of intracellular chloride concentration

Our data are thermodynamically consistent with the idea stated by others that chloride secretion occurs via basolateral chloride entry into the cells

through an $NaKCl_2$ cotransporter. Chloride exits from the cells through an apical membrane CFTR chloride channel (Keeler and Wong, 1986; Fan et al., 1992; Kokko et al., 1997). If we assume that furosemide completely blocks chloride entry while assuming no exit step across the basolateral membranes, then chloride must be at electrochemical equilibrium across the apical membrane chloride channels. Under these conditions, chloride plays no part in determining apical membrane voltage (V_a). At very low Na^+ transport rates where apical membrane voltage must be close to or greater than 100 mV, as expected with the transcellular Thévenin E_{Na} that averaged 112.5 mV, and which can be estimated independently from the quotient of single channel Na^+ current and single channel conductance (~0.5 pA/5 pS = 100 mV) (Helman and Baxendale, 1990; Păunescu et al., 2000b), we calculated that intracellular chloride concentration in the pool of chloride that communicates with the apical membrane is roughly near 2.0 mEq/l (extracellular chloride concentration is 106.8 mM) in amiloride- and furosemide-treated tissues.

From the time-dependent decrease of the I_{sc}^{amil} caused by furosemide, the time constant for loss of chloride from the tissues averaged 3.4 ± 0.7 min (n = 3). By integration of the furosemide-related relaxation of the chloride current transient, we estimated that the loss of chloride from the tissues through apical membranes was 2.7 ± 0.3 nEq/cm^2. If intracellular volume is ~1.0 μl/cm^2 (assuming 80% cell water and average cell thickness of 12 μm) (Butterworth et al., 2001), the change of intracellular chloride concentration due to apical membrane exit would be 2.7 ± 0.3 mM, so that intracellular chloride concentration before treating the tissues with furosemide would be near 4.7 ± 0.3 mM, and higher if chloride also leaves the cells through a basolateral membrane electroneutral transporter(s). In this regard it is important to note that the absence of step changes of current (and thus, conductance) in response to furosemide requires that furosemide inhibits basolateral membrane chloride entry through electroneutral transporters. Because the electrochemical potential difference driving Cl^- out of the cells is the same across both apical and basolateral membranes in short-circuited epithelia, and chloride is secreted, apical membrane conductance to chloride must at a minimum be greater than basolateral membrane chloride conductance if a basolateral membrane conductance to chloride exists at all. To the extent that the basolateral membrane resistance, R_b, of PGE_2-treated tissues averaged near 4 k$\Omega \cdot$ cm^2 and to the extent that this resistance is dominated by the basolateral membrane K^+ conductance, it should be clear that if a basolateral membrane conductance to chloride existed, its value both in absolute terms and in relative terms compared to an apical membrane chloride resistance of 1.5 k$\Omega \cdot$ cm^2 would be small and practically negligible in determining the rates of chloride secretion.

To estimate the loss of cell chloride following PGE_2 we integrated the time-dependent changes of chloride current after PGE_2 assuming constancy of basolateral membrane chloride entry, which introduces some uncertainty in such calculations. Loss of apical membrane chloride caused by PGE_2 averaged 5.5 ± 0.6 nEq/cm^2 with a decrease of intracellular chloride concentration of 5.5 mM. Hence, the chloride concentration within the cells at the time the tissues were treated with PGE_2 was roughly 10.3 ± 0.8 mM. For chloride secretion in amiloride-blocked tissues to have occurred, apical membrane voltage must have exceeded the Nernst potential difference for chloride, which would have been near 60 mV at room temperature. With apical membrane voltage in amiloride-blocked tissues near 100 mV, rapid activation of chloride conductance would result in chloride secretion and loss of cell chloride due to a relatively large net electrochemical potential driving force upon rapid activation of the chloride conductance and secondary dissipation of the driving force to near 3 mV at the steady state when chloride is redistributed toward, but not to electrochemical equilibrium, thereby accounting for the secondary decline of the I_{sc}^{amil} to its steady-state rate of chloride secretion.

Which membrane is rate-limiting for chloride secretion?

The above characteristics of chloride transport in A6 epithelia argue in favor of the idea that chloride secretion is essentially rate-limited at the basolateral membrane. Regardless of the modes of chloride transport at basolateral membranes, fundamental considerations of the laws and theorems of electrical circuit theory require that chloride secretion measured as $I_{sc}^{amil} = (E_a + E_b)/(R_a + R_b)$, where E_a and E_b are the respective Thévenin emfs of apical and basolateral membranes. Thus, regardless of the rates of current or chloride secretion dictated by the values of emf, the chloride current activated by PGE_2 would be limited principally by the R_b in A6 epithelia because $R_b > R_a$, as indicated in Results for the conditions of our experiments.

We gratefully acknowledge the excellent work of A. L. Helman in the growth and preparation of the A6 epithelia, the care of our tissue culture facility, and assistance in preparation of this manuscript.

We also gratefully acknowledge financial support from the National Institute of Diabetes and Digestive and Kidney Diseases Grant DK30824, the University of Illinois at Urbana-Champaign Campus Research Board, and postdoctoral fellowship support to T. G. Păunescu from the National Kidney Foundation and its Illinois affiliate.

REFERENCES

Abramcheck, F. J., W. Van Driessche, and S. I. Helman. 1985. Autoregulation of apical membrane Na^+ permeability of tight epithelia. Noise analysis with amiloride and CGS 4270. *J. Gen. Physiol.* 85:555–582.

Atia, F., W. Zeiske, and W. Van Driessche. 1999. Secretory apical Cl^- channels in A6 cells: possible control by cell Ca^{2+} and cAMP. *Pflugers Arch.* 438:344–353.

Awayda, M. S., W. Van Driessche, and S. I. Helman. 1999. Frequency-dependent capacitance of the apical membrane of frog skin: dielectric relaxation processes. *Biophys. J.* 76:219–232.

Baxendale-Cox, L. M., R. L. Duncan, X. Liu, K. Baldwin, W. J. Els, and S. I. Helman. 1997. Steroid hormone-dependent expression of blocker-sensitive ENaCs in apical membranes of A6 epithelia. *Am. J. Physiol. Cell Physiol.* 273:C1650–C1656.

Brazy, P. C., and R. B. Gunn. 1976. Furosemide inhibition of chloride transport in human red blood cells. *J. Gen. Physiol.* 68:583–599.

Butterworth, M. B., S. I. Helman, and W. J. Els. 2001. cAMP-sensitive endocytic trafficking in A6 epithelia. *Am. J. Physiol. Cell Physiol.* 280:C752–C762.

Chalfant, M. L., B. Coupaye-Gerard, and T. R. Kleyman. 1993. Distinct regulation of Na^+ reabsorption and Cl^- secretion by arginine vasopressin in the amphibian cell line A6. *Am. J. Physiol. Cell Physiol.* 264: C1480–C1488.

Els, W. J., and S. I. Helman. 1981. Vasopressin, theophylline, PGE_2, and indomethacin on active Na transport in frog skin: studies with microelectrodes. *Am. J. Physiol. Renal Physiol.* 241:F279–F288.

Els, W. J., and S. I. Helman. 1997. Dual role of prostaglandins (PGE_2) in regulation of channel density and open probability of epithelial Na^+ channels in frog skin (*R. pipiens*). *J. Membr. Biol.* 155:75–87.

Fan, P. Y., M. Haas, and J. P. Middleton. 1992. Identification of a regulated Na/K/Cl cotransport system in a distal nephron cell line. *Biochim. Biophys. Acta Bio-Membr.* 1111:75–80.

Hall, W. J., J. P. O'Donoghue, M. G. O'Regan, and W. J. Penny. 1976. Endogenous prostaglandins, adenosine 3′:5″-monophosphate and sodium transport across isolated frog skin. *J. Physiol. (Lond).* 258: 731–753.

Helman, S. I., and L. M. Baxendale. 1990. Blocker-related changes of channel density. Analysis of a three-state model for apical Na channels of frog skin. *J. Gen. Physiol.* 95:647–678.

Helman, S. I., and X. Liu. 1997. Substrate-dependent expression of Na^+ transport and shunt conductance in A6 epithelia. *Am. J. Physiol. Cell Physiol.* 273:C434–C441.

Helman, S. I., X. Liu, K. Baldwin, B. L. Blazer-Yost, and W. J. Els. 1998. Time-dependent stimulation by aldosterone of blocker-sensitive ENaCs in A6 epithelia. *Am. J. Physiol. Cell Physiol.* 274:C947–C957.

Helman, S. I., and T. G. Păunescu. 1998. Regulation of epithelial Na^+ channels (ENaCs) by prostaglandins and cAMP/PKA in A6 epithelia. *J. Am. Soc. Nephrol.* 9:35*a*. (Abstr.).

Helman, S. I., and S. M. Thompson. 1982. Interpretation and use of electrical equivalent circuits in studies of epithelial tissues. *Am. J. Physiol. Renal Physiol.* 243:F519–F531.

Keeler, R., and N. L. M. Wong. 1986. Evidence that prostaglandin E_2 stimulates chloride secretion in cultured A6 renal epithelial cells. *Am. J. Physiol. Renal Physiol.* 250:F511–F515.

Koeppen, B. M., K. W. Beyenbach, W. H. Dantzler, and S. I. Helman. 1980. Electrical characteristics of snake distal tubules: studies of I-V relationships. *Am. J. Physiol. Renal. Physiol.* 239:F402–F411.

Kokko, K. E., P. S. Matsumoto, B. N. Ling, and D. C. Eaton. 1994. Effects of prostaglandin E_2 on amiloride-blockable Na^+ channels in a distal nephron cell line (A6). *Am. J. Physiol. Cell Physiol.* 267:C1414–C1425.

Kokko, K. E., P. S. Matsumoto, Z. R. Zhang, B. N. Ling, and D. C. Eaton. 1997. Prostaglandin E_2 increases 7-pS Cl^- channel density in the apical membrane of A6 distal nephron cells. *Am. J. Physiol. Cell Physiol.* 273:C548–C557.

Lambert, A., and A. G. Lowe. 1980. Chloride-bicarbonate exchange in human red cells measured using a stopped flow apparatus. *J. Physiol.* 306:431–443.

Liu, X., W. J. Els, and S. I. Helman. 1995. Aldosterone increases apical membrane capacitance of A6 epithelia. *FASEB J.* 9:64*a*. (Abstr.).

Liu, X., and S. I. Helman. 1998. Time-dependent increases of apical membrane capacitance of A6 epithelia caused by aldosterone. *FASEB J.* 12:123*a*. (Abstr.).

Macchia, D. D., and S. I. Helman. 1979. Transepithelial current-voltage relationships of toad urinary bladder and colon. Estimates of ENa and shunt resistance. *Biophys. J.* 27:371–392.

Marunaka, Y., and D. C. Eaton. 1991. Effects of vasopressin and cAMP on single amiloride-blockable Na channels. *Am. J. Physiol. Cell Physiol.* 260:C1071–C1084.

Matsumoto, P. S., L. Mo, and N. K. Wills. 1997. Osmotic regulation of Na^+ transport across A6 epithelium: interactions with prostaglandin E_2 and cyclic AMP. *J. Membr. Biol.* 160:27–38.

Niisato, N., and Y. Marunaka. 1997. Regulation of Cl^- transport by IBMX in renal A6 epithelium. *Pflugers Arch.* 434:227–233.

Noland, T. D., C. E. Carter, H. R. Jacobson, and M. D. Breyer. 1992. PGE_2 regulates cAMP production in cultured rabbit CCD cells: evidence for dual inhibitory mechanisms. *Am. J. Physiol. Cell Physiol.* 263: C1208–C1215.

Păunescu, T. G. 1999. Regulation of Sodium Transport in A6 Epithelia by Prostaglandin E_2. Ph.D. Dissertation. University of Illinois at Urbana-Champaign, Urbana, IL.

Păunescu, T. G., B. L. Blazer-Yost, and S. I. Helman. 2000a. Role of LY294002 inhibitable PI3-kinase in cAMP activation of PKA and Na^+ transport in A6 epithelia. *FASEB J.* 14:96*a*. (Abstr.).

Păunescu, T. G., B. L. Blazer-Yost, C. J. Vlahos, and S. I. Helman. 2000b. LY-294002-inhibitable PI 3-kinase and regulation of baseline rates of Na^+ transport in A6 epithelia. *Am. J. Physiol. Cell Physiol.* 279: C236–C247.

Păunescu, T. G., and S. I. Helman. 1997. Dual role of prostaglandin E_2 in regulation of Na^+ transport in A6 epithelia. *Biophys. J.* 72:230*a*. (Abstr.).

Păunescu, T. G., and S. I. Helman. 1998. cAMP regulation of channel density and open probability of amiloride-sensitive ENaCs of A6 epithelia. *FASEB J.* 12:122*a*. (Abstr.).

Păunescu, T. G., and S. I. Helman. 2000. Impedance analysis of PGE_2 activation of apical membrane Cl^- conductance in A6 epithelia. *FASEB J.* 14:596*a*. (Abstr.).

Păunescu, T. G., and S. I. Helman. 2001. cAMP activation of apical membrane Cl^- channels: theoretical considerations for impedance analysis. *Biophys. J.* 81:838–851.

Păunescu, T. G., X. Liu, and S. I. Helman. 1997. Nonhormonal regulation of apical membrane sodium transport in A6 epithelia. *FASEB J.* 11:8*a*. (Abstr.).

Perkins, F. M., and J. S. Handler. 1981. Transport properties of toad kidney epithelia in culture. *Am. J. Physiol. Cell Physiol.* 241:C154–C159.

Schlondorff, D., and J. A. Satriano. 1985. Interactions of vasopressin, cAMP, and prostaglandins in toad urinary bladder. *Am. J. Physiol. Renal Physiol.* 248:F454–F458.

Sonnenburg, W. K., and W. L. Smith. 1988. Regulation of cyclic AMP metabolism in rabbit cortical collecting tubule cells by prostaglandins. *J. Biol. Chem.* 263:6155–6160.

Stoddard, J. S., E. Jakobsson, and S. I. Helman. 1985. Basolateral membrane chloride transport in isolated epithelia of frog skin. *Am. J. Physiol. Cell Physiol.* 249:C318–C329.

Yanase, M., and J. S. Handler. 1986. Adenosine 3′,5′-cyclic monophosphate stimulates chloride secretion in A6 epithelia. *Am. J. Physiol. Cell Physiol.* 251:C810–C814.

Yonath, J., and M. M. Civan. 1971. Determination of the driving force of the Na^+ pump in toad bladder by means of vasopressin. *J. Membr. Biol.* 5:366–385.

Zeiske, W., F. Atia, and W. Van Driessche. 1998. Apical Cl^- channels in A6 cells. *J. Membr. Biol.* 166:169–178.